NJC

Accepted Manuscript

This article can be cited before page numbers have been issued, to do this please use: L. Wang, L. Yang, L. Li and D. Cao, *New J. Chem.*, 2016, DOI: 10.1039/C6NJ00192K.

ROYAL SOCIETY OF CHEMISTRY

www.rsc.org/njc

View Article Online
DOI: 10.1039/C6NJ00192K

Synthesis and highly sensitive detection of water content in THF using a novel solvatachromic AIE polymer containing diketopyrrolopyrrole and triphenylamine

Lingyun Wang [a]*, Lingling Yang[a], Lin Li [b]*, Derong Cao [a]

[a] School of Chemistry and Chemical Engineering, State Key Laboratory of Luminescent Materials and Devices, South China University of Technology, Guangzhou, China, 510641

[b] School of Food Science and Engineering, South China University of Technology, Guangzhou, China, 510641

*Corresponding author: Tel. +86 20 87110245; fax: +86 20 87110245. E-mail: lingyun@scut.edu.cn; felinli@scut.edu.cn

View Article Online
DOI: 10.1039/C6NJ00192K

Abstract:

A novel electron donor-acceptor polymer (**N1**) containing diketopyrrolopyrrole as electron acceptor and triphenylamine as electron donor has been designed and synthesized. **N1** is shown to possess the remarkable dual properties of solvatochromism and aggregation-induced emission (AIE). Importantly, **N1** is found to serve as a fluorescent indicator for the qualitative and quantitative detection of low-level water in THF. Moreover, the quaternization of **N1** by CH_3I gave ammonium-salt **P1**. A selective fluorescence turn-on probe for bovine serum albumin (BSA) detection and quantification is developed by taking advantage of the aggregating process of **P1**. It is found that the intrinsic weak fluorescence of **P1** in DMSO/PBS (1:1, v/v) increases to 2.9-fold after addition of 50 μM BSA through electrostatic complexation and hydrophobic interaction.

Keywords: Aggregation induced emission (AIE), Diketopyrrolopyrrole, triphenylamine, Intramolecular charge transfer (ICT), Solvatochromism

View Article Online
DOI: 10.1039/C6NJ00192K

1. Introduction

Aggregation-induced emission (AIE) is a newly developed phenomenon that is exactly opposite to the aggregation-caused quenching (ACQ) effect observed with some conventional luminophores. Luminogens with AIE characteristic have emerged as promising materials for fabricating bio-probes for their incredible emission efficiency upon interaction with biomolecules in aqueous solutions.[1] The water-soluble and red-emitting AIE-active systems are highly desirable due to their minimal photo-damage to living cells and deep tissue penetration.[2] In principle, red-emitting dyes come from a narrowed energy-gap, which can be realized by two strategies. One is by extending the π -conjugation system such as those observed for large planar conjugated molecules. However, planar structures often present ACQ effect due to intermolecular π–π stacking. Another is by introducing strong electron donor (D) and acceptor (A) groups into a conjugated luminogen to concomitantly drive up the HOMO and pull down the LUMO.[3] Moreover, the building of electron donor–acceptor structure is an effective way to improve luminescent property of fluorophores,[4, 5] which increases its dipole moment and as a result the molecule becomes sensitive to its environment.

Diketopyrrolopyrrole (DPP) dyes offer distinctive advantages relative to other organic dyes, including high fluorescence quantum yields, good light and thermal stability. In particular, DPP dyes can emit brilliant red-fluorescence after specific structural modification, which makes them better to be applied in biosensors. Therefore, DPP would be a good candidate for developing red-emitting material.

View Article Online
DOI: 10.1039/C6NJ00192K

Significant advancements have been made in the development of new fluorescent probes based on DPP in recent years.[6] However, it is a great challenge to sustain the efficient emission of DPP-based compounds in aggregated states due to the serious intermolecular π – π stacking. To overcome this problem, it is a rational strategy to attach bulky or AIE substituents onto DPP to hinder the ACQ effect, but still very limited.[7] In our recent work, two new red-emitting AIE-active DPP compounds were synthesized, where the introduction of anthranone successfully converted DPP dye from ACQ to AIE.[8]

On the other hand, triphenylamine (TPA) has recently become a material with great prospects due to its AIE properties.[9] Moreover, TPA as a conventional electron donating group is frequently employed to generate various compounds with electron donor–acceptor structure.[10-12] Recently, Liu's and Hua's groups investigated biocompatible nanoparticles based on DPP with aggregation-induced red/NIR emission for *in vivo* two-photon fluorescence imaging, where propeller-like starburst TPA as a strong donor tethered to the central DPP acceptor *via* vinyl arm.[13] However, most of the AIE systems especially those containing TPA moieties developed so far displaying both AIE and solvatochromism are still quite limited and possess low-molecular weights. For practical applications, the polymer with high molecular weight and good film-forming capacity would be desirable. Preparation of polymers with AIE features may help to solve ACQ problem and meanwhile impart polymers with new properties and practical applications. Moreover, due to the "signal amplification effect" of the conjugated polymer chains, AIE polymers enjoy superior

View Article Online
DOI: 10.1039/C6NJ00192K

sensitivity when work in the application of chemo- and bio-sensors compared with AIE small molecules. At the same time, the superior stability and strong emission efficiency of polymer enable long-term tracking of the cell for bioimaging applications. Therefore, the development of long-wavelength AIE-active polymers with pronounced solvatochromic effect and probably higher sensitivity and larger responses to external stimuli, is still a challenging task.

Herein, a novel conjugated polymer (**N1**) has been designed and synthesized, as shown in Scheme 1. In the molecular design, the TPA group is introduced because it can act not only as a strong electron-donor group to induce intramolecular charge transfer (ICT) transition but also as an activator for AIE. It was thus expected that **N1** possesses intense ICT effect, which bestow **N1** with pronounced solvatochromism. Indeed, **N1** exhibit strong solvent-dependent fluorescence and AIE behaviour. Importantly, the emission band of **N1** was effectively quenched upon addition of increasing concentration of water in THF. So, **N1** can serve as a fluorescent indicator for the qualitative and quantitative detection of low-level water in THF. **N1** was further treated with CH_3I at room temperature to afford its ionized product (**P1**). Due to the multivalent interactions of **P1** with negative bovine serum albumin (BSA), **P1** shows superamplification effect in the emission enhancement of its nanoaggregates and works as sensitive and selective fluorescence "turn-on" probe for BSA quantitation.

2. Experimental

View Article Online
DOI: 10.1039/C6NJ00192K

2.1. Chemicals and instruments

Tetrahydrofuran (THF) and dioxane was distilled under normal pressure from sodium under argon immediately prior to use. Other solvents and chemicals were obtained from commercially available resources without further purification. Compound **3** was synthesized by the published paper .[14]

^{1}H and ^{13}C NMR spectra were measured on Bruker Avance III 400 MHz (in $CDCl_3$ or in DMSO-d_6, TMS as internal standard). Fourier transform infrared (FT-IR) spectra were recorded on an RFX-65A (Analect Co.) spectrometer. The UV-vis absorption spectra were recorded using a Helios Alpha UV-Vis scanning spectrophotometer. Fluorescence spectra were obtained with a Hitachi F-4500 FL spectrophotometer with quartz cuvette (path length = 1cm). The fluorescence spectra were obtained by excitation at 500 nm and the excitation and emission slit widths were 10 nm and 20 nm, respectively.

*2.2. Synthesis of **Monomer 1***

Compound **3** (0.223 g, 0.5 mmol), KOAc (0.276 g, 2 mmol), bis(pinacolato)diboron (507 mg, 2 mmol) and $Pd(dppf)_2Cl_2$ were mixed in anhydrous dioxane. Then the mixture was heated under reflux for 24 h under argon. After cooling, the solvent was removed under reduced pressure. The crude produce was purified by column chromatography (petroleum ether: CH_2Cl_2: ethyl acetate =5:4:0.3) on silica gel to afford orange solid in 46.2% yield. ^{1}H NMR ($CDCl_3$, 400 MHz, δ, ppm): 8.00 (d, *J*=8.0 Hz, 4H), 7.80 (d, *J*=8.0 Hz, 4H), 3.77 (t, *J*=4.0 Hz, 4H), 3.34 (t,

View Article Online
DOI: 10.1039/C6NJ00192K

J=4.0 Hz, 4H), 1.79-1.76 (m, 4H), 1.68-1.55 (m, 6H), 1.39 (s, 24H), 1.28-1.23 (m, 6H). ^{13}C NMR ($CDCl_3$, 100 MHz, δ, ppm): 162.5, 162.4, 148.4, 147.4, 135.1, 132.3, 130.5, 130.0, 127.7, 126.9, 125.9, 110.2, 110.0, 84.2, 41.6, 33.6, 32.5, 29.2, 27.6, 25.8, 24.9. TOF-MS m/z: 867.289 $[M+H]^+$.

Monomer 2 was synthesized according to the previous literature.[15] ^{1}H NMR ($CDCl_3$, 400 MHz, δ, ppm): 7.31 (d, *J*=8.0 Hz, 4H), 7.03 (d, *J*=8.0 Hz, 2H), 6.90 (d, *J*=8.0 Hz, 4H), 6.86 (d, *J*=8.0 Hz, 2H), 3.94 (t, *J*=8.0 Hz, 2H), 1.82-1.76 (m, 2H), 1.49-1.46 (m, 2H), 1.38-1.36 (m, 4H), 0.93 (t, *J*=8.0 Hz, 3H). ^{13}C NMR ($CDCl_3$, 100 MHz, δ, ppm): 156.4, 146.9, 139.5, 132.2, 127.4, 124.3, 115.6, 114.5, 68.3, 31.6, 29.3, 25.8, 22.6, 14.1. TOF-MS m/z: 502.892 $[M+H]^+$.

Synthesis of **N1**.

To a solution of THF (15 mL), **Monomer 1** (216 mg, 0.25 mmol), **Monomer 2** (125.75 mg, 0.25 mmol) and $Pd(Pph_3)_4$ (28.9 mg, 0.025 mmol) were added. The mixture was deoxygenated by purging with purified N_2 gas and then K_2CO_3 (2 mol/L, 4.5 mL) was injected. The mixture was heated at 50°C for 18 h under N_2. After cooled, the mixture was poured into water, extracted with CH_2Cl_2 three times and then washed with water and EDTA solution in sequence. The concentrated solution was dropwise added into methanol. The precipitate was collected by filtration from methanol and dried under vacuum to yield **N1** (177 mg, 72%) as a deep red solid. GPC: M_w= 9751, M_n=7548, PDI=1.29. ^{1}H NMR ($CDCl_3$, 400 MHz, δ, ppm): 7.90-7.88 (m, 2H), 7.76-7.72 (m, 4H), 7.57-7.51 (m, 2H), 7.40-7.33 (m, 4H), 7.20-6.86 (m, 8H),

View Article Online
DOI: 10.1039/C6NJ00192K

3.97-3.94 (m, 2H), 3.83 (br, 2H), 3.30 (br, 6H), 1.81-1.67 (m, 10H), 1.45-1.26 (m, 14H), 0.91 (br, 3H).

The ionization of **N1** was realized by adding 1 mL trimethylamine to a solution of **N1** (100 mg) in 10 mL $CHCl_3$ and stirring for 24 h at room temperature. The polymer precipitate was collected and washed with THF, and then dried under vacuum to yield **P1** (85 mg). ^{1}H NMR (DMSO-d_6, 400 MHz, δ, ppm): 8.18-6.62 (m, 20H), 4.04-3.61 (m, 10H), 3.02-2.78 (m, 24H), 1.49-0.91 (m, 21H).

2.3. Preparation of aggregates

Stock solutions of **N1** were prepared in DMF, with a concentration of 0.1 mM. An aliquot (1 mL) of the stock solution was transferred to a 25 mL erlenmeyer flask. After adding an appropriate amount of DMF, water was added dropwise under vigorous stirring to furnish 10 μM solution with water fractions (f_w) of 0–90 vol %.

2.4 Discrimination of BSA

The discrimination of BSA was carried out in a solvent system of DMSO:PBS=1:1 (v/v). The fluorescence BSA titrations were carried out by sequentially adding 0-200μL aliquots of BSA solution (5×10^{-4} M) to a 20μL stock solution of **P1** followed by addition of 980 μmL DMSO and an aqueous PBS buffer to acquire a solution of 2.0 mL.

3. Results and discussion

3.1. Synthesis and structural characterization

View Article Online
DOI: 10.1039/C6NJ00192K

The synthetic routes of **Monomer 1** are shown in Scheme 1, and the key compound **3** was synthesized according to the literature.[14] **Monomer 1** bearing two pinacol boronate groups was accomplished by the Pd-catalyzed Suzuki reaction of **3** with bis(pinacolato)diboron in the presence of catalytic amounts of Pd(dppf)Cl_2 and potassium acetate. **Monomer 2** was synthesized according to the previous literature.[15] **Monomer 1** and **Monomer 2** were carefully characterized by proton and carbon nuclear magnetic resonance spectroscopy (^{1}H, ^{13}C NMR) and high resolution mass spectroscopy (MS-TOF) (see the ESI, Figs. S1-S2 for the details). The neutral precursor polymer **N1** was synthesized by Suzuki coupling reaction of **Monomer 1** and **Monomer 2**. As shown in Fig.1, **Monomer 1** shows a strong singlet at 1.39 ppm corresponding to the methyl proton of boryl. However, this singlet does not appeared in the ^{1}H NMR spectrum of **N1**, implying the successful polymerization of **Monomer 1** and **Monomer 2**. **N1** is soluble in common organic solvents such as dichloromethane, chloroform, and THF. The ionization of **N1** was realized by treating **N1** with trimethylamine at room temperature for 24 h to generate **P1** in order to improve the water solubility and provide the positive charged ammonium binding sites for the electrostatic interaction between the **P1** and negative analytes. **P1** is readily soluble in dimethyl formamide (DMF) and dimethyl sulfoxide (DMSO).

*3.2 Solvatochromic effect of **N1***

TPA is well-known to be very effective π-electron-donating group with high donor strength. In the TPA–DPP structural framing of **N1**, TPA was the donor part while

View Article Online
DOI: 10.1039/C6NJ00192K

DPP served as the acceptor part. Consequently, the excitation of the ICT state induced a charge shift from the donor to the acceptor part, which would cause significant solvatochromism. Fig. 2a exhibits the normalization absorption of **N1** in the different solvent. For **N1**, the absorption spectral maximum is dependent on the solvent polarity; the magnitude of the solvatochromic shift from ethyl acetate (499 nm) to $CHCl_3$ (522 nm) is 23 nm. Thus, various colors in different solvents are present (Fig. 2b).

As the solvent polarity increases, this interaction becomes stronger, resulting in emission at lower energies or longer wavelengths. With increasing the solvent polarity, **N1** exhibits polarity-dependent solvatochromism of fluorescence (Fig. 3a). In dioxane and toluene, **N1** emits strong yellow fluorescence with the same emission peak at 602 nm. The emission maxima further red-shifts to 620, 625 and 611 nm in CH_2Cl_2, $CHCl_3$ and THF, respectively. However, blue-shifted maxima emission peaks at 576, 598 and 591 nm in acetone, ethyl acetate and DMF are observed, respectively. In more polar solvents such as DMF, the fluorescence of **N1** is nearly completely quenched. Such changes in fluorescence spectra indicate that the excited state has a larger dipole moment than the ground state. Accordingly, **N1** in various solvents exhibited dramatic fluorescent color variations under illumination with 365 nm light. Strong yellow emission in toluene and dioxane, weak red-orange emission in chloroform, CH_2Cl_2, and THF were observed. While in more polar solvents such as DMF and acetonitrile, the emission becomes very weak due to the promotion of ICT process (Fig. 3b).

View Article Online
DOI: 10.1039/C6NJ00192K

*3.3 AIE behaviours of **N1***

To investigate the AIE properties of **N1**, we employed anhydrous DMF as the good solvent and water as the poor solvent. The emission spectra of **N1** in DMF and DMF/water mixture solutions were recorded (Fig. 4a). Clearly, the fluorescent intensity of **N1** is rather weak in pure DMF solution. However, the fluorescent intensity increases dramatically when the water content is above 80%. As the water content reachs 90%, the photoluminescence intensity is boosted to the maximum. Eventually, the emission intensity of **N1** is approximately 7 folds higher than its molecularly dispersed species in DMF (Fig. 4b). The apparent emission enhancement of **N1** is thus induced by aggregation, verifying its AIE nature owing to the restricted intramolecular motions mechanism: large amount of water resulted in formation of aggregated nanoparticles, which subsequently impeded the intramolecular rotations of the aromatic rotors of **N1** and endowed the aggregates with intense emission.

Moreover, compared to the pure DMF solution of **N1**, the emission maximum of the aggregates blue-shifted from 625 nm to 600 nm, and the emission color changed from red to orange (Fig. 4c). The weak and redder emission in pure DMF solution implied the existence of large-amplitude relaxation in the excited state, such as intramolecular charge transfer (ICT). Nevertheless, aggregation forced the molecules to reside in an apolar environment which is unfavourable for ICT process, resulting in the blue shift of the emission maximum and was also helpful for the light emission. In contrast to the fluorescence, the absorption spectra of **N1** were red-shifted (508 to 522 nm) and broadened upon addition of water, due to the nanoaggregated structure of the

View Article Online
DOI: 10.1039/C6NJ00192K

molecules (see the ESI, Fig. S3). Meanwhile, the level-off tails in the visible region of the absorption spectra clearly indicated the formation of aggregates.

*3.4 Detection of low-level water in THF by **N1***

The qualitative and quantitative detection of low-level water content as impurity in organic solvents is of great significance in several fields of chemistry and industrial processes such as pharmaceutical manufacturing, food processing, paper production, biomedical and environmental monitoring.[16] Particularly using fluorescence methods, parameters such as lifetime, intensity and wavelength ratiometric sensing have been widely studied and applied for detection of water content in organic solvents.[17]

Clearly, the fluorescence emission of **N1** is highly sensitive to solvent polarity according to the above discussions. Therefore, we further investigated its emission behaviour in non-hydrogen-bond donating water-miscible solvents, *i.e.*, THF. As shown in Fig. S4 (see the ESI), the absorption spectra of **N1** in THF solution underwent slight changes from pure THF to THF containing 10% (v/v) water, indicating that neither solvent polarity nor hydrogen bonding has a significant influence on the absorption spectra. In contrast, upon further addition of water in THF solution, the emission of **N1** is effectively quenched and that of **N1** is gradually diminished along with blue-shift from 603 nm to 590 nm (Fig. 5a). These phenomena can be attributed to the cooperative effect of the solvent polarity and the ICT effect. Fig. 5b shows in details how the measured fluorescent intensity changes as a function of water content in the THF solution of **N1**. As can be seen from the graph (Fig. 5b),

View Article Online
DOI: 10.1039/C6NJ00192K

the fluorescent intensity of **N1** decreases dramatically when the water content is below 2.00% (v/v): the reduction in relative fluorescence intensity reaches nearly 53%, whereas such effect became moderate when the water content is higher than 2.00% (v/v). More importantly, the fluorescent intensity of **N1** as a function of water content shows a good linear relationship below 2.00% (v/v), and the detection limit of **N1** for water is determined as 0.005% in THF. In comparison with reported solvatochromic dyes for the detection of water in organic solvents,[18, 19] the detection limit of **N1** is high, demonstrating that **N1** is sensitive to low-level water content in THF. It can be also utilized to quantitatively detect low-level water content in organic solvents.

*3.5 The photophysical properties of **P1***

The addition of p oor solvent (such as THF or methanol) to the solution of **P1** in DMSO fails to make **P1** aggregate, possibly because of its amphiphilic nature.[20] Hence, the increasing viscosity is investigated to study whether **P1** possesses AIE effect. As shown in Fig. 6, the emission intensity of **P1** in glycerol/DMSO mixture (9:1, v/v) is about 1.15-fold higher than that in DMSO, which implies that **P1** is AIE-active. These phenomena occur because high viscosity can hamper intramolecular rotation, leading to the closure of the nonradiative decay channel and thus enhanced fluorescence emission.

*3.6 **P1** serves as a probe for detecting BSA*

View Article Online
DOI: 10.1039/C6NJ00192K

The "traditional" polymer bioprobes usually operate in a light "turn-off" mode due to the emission quenching caused by the electron and/or energy transfers between the polymer chains and the bioanalytes. It will be better if the bioprobes can work in a fluorescence "turn-on" mode, which enjoys such advantages as high detection sensitivity, reduced false-positive signals, and visual recognition or discrimination with the naked eyes.

P1 is positively charged and should show affinity toward negatively charged biopolymers. Bovine serum albumin (BSA), which contains hydrophobic binding sites in its native folding structure and has a negative charge (the isoelectric point is about 4.7) in water medium at neutral pH, can bind with **P1** through electrostatic and hydrophobic interaction. Considering the optical properties of **P1**, we infer **P1** would be suitable for application as a fluorescence turn-on probe for BSA based on controllable aggregation processes through hydrophobic effect and electrostatic interaction and tuning the π…π stacking interactions by BSA. To explore the possibility of utilizing **P1** for protein assay, its emission spectra in the absence and presence of BSA are measured. Fig. 7 shows the FL spectral changes in **P1** before and after the addition of BSA. **P1** is weakly luminescent in DMSO/PBS (v/v, 1/1); however, the FL intensity of the buffer solution of **P1** increases gradually when BSA is introduced. For instance, the FL intensity of **P1** at 570 nm is enhanced to 2.9-fold after the concentration of BSA reaches 50 μM.

In the BSA concentration range of 0-1 μM, the I/I_0-1 *vs* [BSA] plot follows a linear relationship with an outstanding "goodness-of-fit" (R^2 = 0.994). The detection limit is

View Article Online
DOI: 10.1039/C6NJ00192K

0.0038 μM, demonstrating that **P1** can function as a biological probe for BSA quantification at subppm level. In comparison with reported small molecular AIE system for the detection of BSA [8], the detection limit of **P1** was high. This can be attributed to explanations: (1) the "signal amplification effect" of the conjugated polymer makes **P1** to be more sensitive to BSA; (2) The native BSA contains hydrophobic binding sites such as hydrophobic pockets in folding structures. **P1** has more suitable size and structure to enter the hydrophobic pockets and bind to BSA, which benefit the stronger interaction with BSA.

In order to further verify that the enhancement of the fluorescence intensity of **P1** is ascribed to the formation of aggregates of **P1** with BSA, the corresponding sizes were studied by using dynamic light scattering (DLS) before and after the addition of BSA (Fig. 8). The mean diameter of **P1** in the mixture of DMSO/PBS (v/v, 1/1) is 589 nm while the mean diameter increases to 917 nm as 50 μM BSA is introduced. Moreover, Fig. S5 (see the ESI) demonstrates the changes in the absorption spectrum of **P1** (20 μM) in the absence and presence of BSA. **P1** has absorbance maxima peak at 537 nm. A level-off tail is observed in the presence of BSA, further indicating that the formation of aggregates.

*3.7. The selectivity of **P1** for detecting BSA*

As compared with significant fluorescence response induced by BSA, however, no significant changes in **P1** fluorescence intensity as well as emission maxima peak position is observed after addition of the same concentration of negative charged

View Article Online
DOI: 10.1039/C6NJ00192K

biological species such as alkaline phosphatase (ALP), DNA and other anions (Cl^-, Br^-, I^-, NO_3^-, AcO^-, CO_3^- and PO_4^{3-}) (Fig. 9). The conventional reported protein detection methods exhibit various responses for different proteins [21], which results in poor selectivity. These differences are related to the amino acid sequence, pI, protein structure and the presence of certain side chains that can dramatically alter the proteins response and their hydrophobicity [22]. BSA appears to be the most "hydrophobic" proteins among these proteins/ enzymes used, while ALP, DNA are less 'hydrophobic' proteins and hence have lower binding affnity for **P1**. Herein, in the buffer solutions, the cationic amphiphilic **P1** bind to BSA *via* supramolecular interactions such as electrostatic interaction and the hydrophobic effect. For the native BSA, it contains hydrophobic binding sites such as hydrophobic pockets. When **P1** bind to the hydrophobic regions of BSA chains and enter into the hydrophobic pockets of their folding structures, the intramolecular rotations of **P1** are frozen, inducing them to emit as aggregation does. All these findings suggested that **P1** can serve as a selective probe for discriminating BSA.

4. Conclusions

A diketopyrrolopyrrole and triphenylamine containing conjugated polymer **N1** and its ionized product **P1** were designed and synthesized. **N1** displays ICT fluorescence in different solvents and AIE characteristic. The emission intensity of **N1** is approximately 7 folds higher in DMF/H_2O (1/9, v/v) than its molecularly dispersed species in DMF. Moreover, **N1** could be utilized as a fluorescent probe for the

View Article Online
DOI: 10.1039/C6NJ00192K

qualitative detection of low-evel water content in THF. In particular, the low detection limit (0.005% in THF) enables it a supersensitive water sensor for pratical applications. Furthermore, **P1** can function as a fluorescence "turn on" probe for discriminating BSA. Other biological species bearing negative charge such as DNA, ATP and anions have no significant effect on the fluorescence of **P1**, indicating that **P1** has good selectivity for BSA.

View Article Online
DOI: 10.1039/C6NJ00192K

Acknowledgements

The supports by National Basic Research Program of China (2012CB720801), National Natural Science Foundation of China (No. 21274045), the Fundamental Research Funds for the Central Universities (2015ZZ037) and the Natural Science Foundation of Guangdong Province (2015A030313209, 2016A030311034) are gratefully acknowledged.

View Article Online
DOI: 10.1039/C6NJ00192K

Reference

[1] D. Ding, K. Li, B. Liu, B. Z. Tang, *Acc. Chem. Res.*, 2013, **46**, 112441– 2453.

[2] A. D. Shao, Z. Q. Guo, S. J. Zhu, S. Q. Zhu, P. Shi, H. Tian, W. H. Zhu, *Chem. Sci.*, 2014, **5**, 1383–1389.

[3] (a) X. Y. Shen, W. Z. Yuan, Y. Liu, Q. L. Zhao, P. Lu, Y. G. Ma, I. D. Williams, A. J. Qin, J. Z. Sun, B. Z. Tang, *J. Phys. Chem. C*, 2012, **116**, 10541− 10547, (b) X. Y. Shen, Y. J. Wang, E. G. Zhao, W. Z. Yuan, Y. Liu, P. Lu, A. J. Qin, Y. G. Ma, J. Z. Sun, B. Z. Tang, *J. Phys. Chem. C*, 2013, **117**, 7334 – 7347.

[4] H. Y. Bai, J. H. Qian, H. Y. Tian, W. W. Pan, L. Y. Zhang, W. B. Zhang, *Dyes Pigm.*, 2014, **103**, 1– 8; (b) Y. Liu, X. T. Tao, F. Z. Wang, X. N. Dang, D. C. Zou, Y. Ren, M. H. Jiang, *J. Phys. Chem. C*, 2008, **10**, 3975–3981.

[5] C. L. Chiang, M. T. Wu, D. C. Dai, Y. S. Wen, J. K. Wang, C. T. Chen, *Adv. Funct. Mater.*, 2005, **15**, 231–238.

[6] M. Kaur, D. H. Choi, *Chem. Soc. Rev.*, 2015, **44**, 58−77.

[7] (a) X. Q. Li , X. Zhang, S. Ghosh, F. Würthner, *Chem. Eur. J.*, 2008, **14**, 8074−8078; (b) Y. Che, X. Yang, K. Balakrishnan, J. Zuo, L. Zang, *Chem. Mater.*, 2009, **21**, 2930−2934; (c) Q. Zhao, K. Li, S. Chen, A. Qin, D. Ding, S. Zhang, Y. Liu, B. Liu, J. Z. Sun, B. Z. Tang, *J. Mater. Chem.,* 2012, **22**, 15128−15135; (d) H.T. Zhou, W. Huang, L. Ding, S. Y. Cai, X. Li, B. Li, J. H. Su, *Tetrahedron*, 2014, **70**, 7050−7056; (e) B. Wang, N. N. He, B. Li, S. Y. Jiang, Y. Qu, S. Y. Qu, J. L. Hua, *Aust. J. Chem.*, 2012, **65**, 387–394, (f) X. Y. Shen, Y. J. Wang, H. K. Zhang, A. Qin, J. Z. Sun, B. Z. Tang, *Chem. Commun.*, 2014, **50**, 8747–8750.

View Article Online
DOI: 10.1039/C6NJ00192K

[8] L.Y. Wang, L. L. Yang, D. R. Cao , *Sens. Actuators B*, 2015, **221**, 155–166.

[9] B. Wang, Y. C. Wang, J. L. Hua, Y. H. Jiang, J. H. Huang, S. X. Qian, H. Tian, *Chem. Eur. J.*, 2011, **9**, 2647–2655.

[10] L. J. Chen, Y. J. Cui, X. N. Mei, G. D. Qian, M. Q. Wang, *Dyes Pig.*, 2007, **3**, 293–298.

[11] B. Li, Q. Li, B. Liu, Y. F. Yue, M. X. Yu, *Dyes Pig.*, 2011, **3**, 301–306.

[12] T. C. Lin, W. L. Lin, C. M. Wang, C. W. Fu, *Eur. J. Org. Chem.*, 2011, **5**, 912–921.

[13] Y. T. Gao, G. X. Feng , T. Jiang, C. Goh, L. Ng, B. Liu, B. Li , L. Yang, J. L. Hua, H. Tian, *Adv. Funct. Mater.*, 2015, **25**, 2857–2866.

[14] Z. Qiao, J. B. Peng, Y. Jin, *Polymer*, 2010, **51**, 1016-1023.

[15] S. M. Park, K. S. Yook, W. H. Lee, Y. Hong, J. Y. Lee, *J. Polym. Sci., Part A: Polym. Chem.*, 2013, **51**, 5111–5117.

[16] M. M. F. Choi , O. L. Tse, *Anal. Chim. Acta*, 1999, **378**, 127–134.

[17] (a) Q. Chang, Z. Murtaza, J. R. Lakowicz, G. Rao, *Anal. Chim. Acta*, 1997, **350**, 97–104; (b) A. Hakonen, N. Strömberg, *Analyst*, 2012, 137, 315–321; (b) H. Mishra, V. Misra, M. S. Mehata, T. C. Pant, H. B. Tripathi, *J. Phys. Chem. A*, 2004, **108**, 2346–2352; (c) X. Yang, C. G. Niu, Z. J. Shang, G. L. Shen, R. Q. Yu, *Sens. Actuators B*, 2001, **75**, 43–47; (d) C. M. Rushworth, Y. Yogarajah, Y. Zhao, H. Morgan, C. Vallance, *Anal. Methods*, 2013, **5**, 239–247; (e) Y. Ooyama, A. Matsugasako, Y. Hagiwara, J. Ohshita, Y. Harima, *RSC Adv.*, 2012, **2**, 7666–7668; (f) S. Ishihara, J. Labuta, T. Sikorsky, J. V. Burda, N. Okamoto, H. Abe, K. Ariga, J. P. Hill, *Chem.*

View Article Online
DOI: 10.1039/C6NJ00192K

Commun., 2012, **48**, 3933–3935; (g) A. Hakonen and N. Stro ¨mberg, *Chem. Commun.*, 2011, **47**, 3433–3435.

[18] X. Lou, D. Ou, Q. Li, Z. Li, *Chem. Commun.*, 2012, **48**, 8462–8477.

[19] (a) Y. Zhang, D. Li, Y. Li, J. Yu, *Chem. Sci.*, 2014, **5**, 2710–2716; (b) W. Chen, Z. Y. Zhang, X. Li, H. Agren, J. H. Su, *RSC Adv.*, 2015, **5**, 12191 –12201.

[20] H.G. Lu, B. Xu, Y. J. Dong, F.P. Chen, Y. W. Li, Z. F. Li, J. T. He, H. Li, W. J. Tian, *Langmuir*, 2010, **26**, 6838–6844.

[21] Y.D. Hang, L. Yang, Y. Qu, J.L. Hua , *Tetrahedron Lett.*, 2014, **55**, 6998–7001.

[22] C. Michael, N. K. Puri, *Biochem. J.*, 1992, **282**, 589–593.

View Article Online
DOI: 10.1039/C6NJ00192K

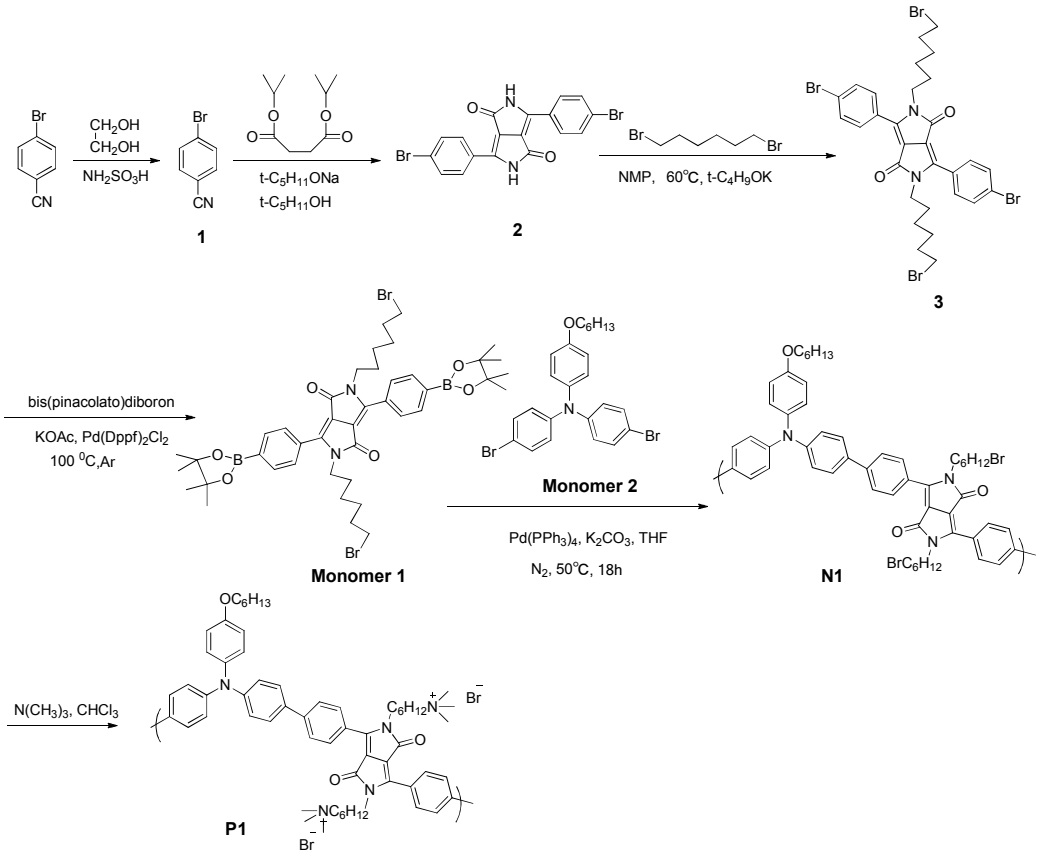

Scheme 1. Synthesis of **N1** and **P1**.

View Article Online
DOI: 10.1039/C6NJ00192K

Figure captions

Fig. 1. The ^{1}H NMR spectra of **Monomer 1, Monomer 2** and **N1**.

Fig. 2. (a) The normalized UV-vis spectra and (b) photographs of **N1** in different solvent.

Fig. 3. (a) The normalized emission spectra of and (b) photographs of **N1** in different solvent under UV irridiation.

Fig. 4 (a) Emission spectra of **N1** (10 μM) in DMF/H_2O (λ_{ex} = 500 nm); (b) Plots of relative emission intensity enhancement factors *versus* water fractions; (c) Emission photographs of **N1** in DMF/H_2O mixtures with different water fractions at 365 nm UV irradiation.)

Fig. 5 (a) Emission spectra of **N1** (10 μM) in THF/H_2O (λ_{ex} = 500 nm); (b) Plots of relative emission intensity (I/I_0) *versus* water fractions.

Fig. 6. Emission spectra of **P1** (20 μM) in various glycerol–DMSO mixture (λ_{ex} = 500 nm)

Fig.7. Emission spectra of **P1** (20 μM) in various amount of BSA (λ_{ex}= 500 nm) in DMSO/PBS mixture (1:1, v/v). Inset: photogragh of **P1** in the presence and absence of BSA).

Fig. 8. Particle size distribution of **P1** (20 μM) in DMSO/PBS mixture (1:1, v/v) in the absence (a) and presence (b) of 50 μM BSA.

Fig.9. The fluorescence spectra of **P1** (10 μM) in presence of 50 μM DNA, ATP and anions.

View Article Online
DOI: 10.1039/C6NJ00192K

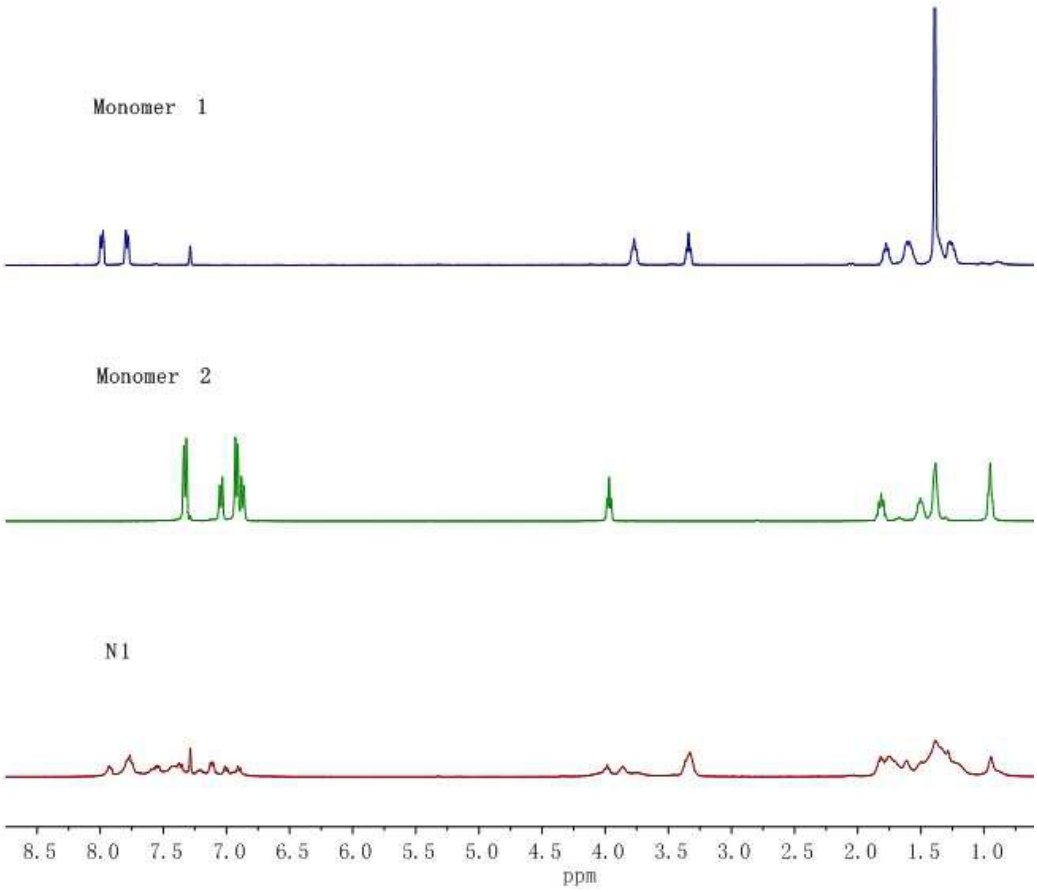

Fig. 1. The ^{1}H NMR spectra of **Monomer 1, Monomer 2** and **N1**.

View Article Online
DOI: 10.1039/C6NJ00192K

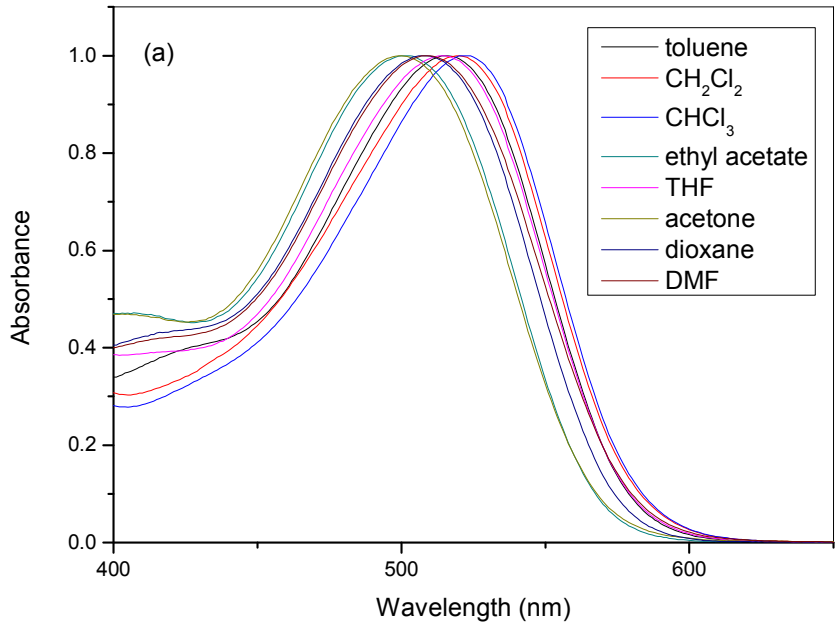

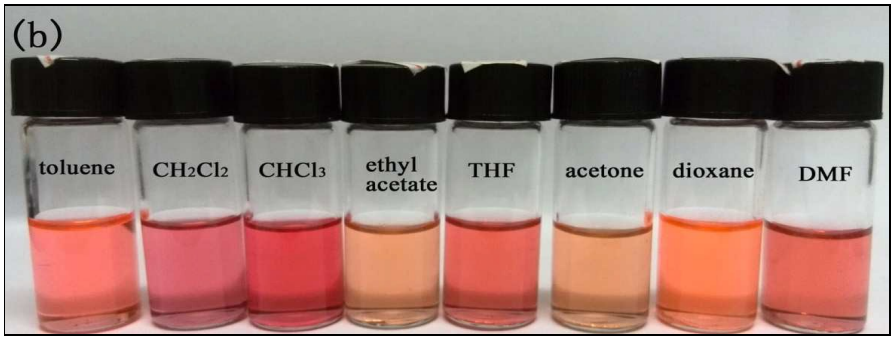

Fig. 2. (a) The normalized UV-vis spectra and (b) photographs of **N1** in different solvent.

View Article Online
DOI: 10.1039/C6NJ00192K

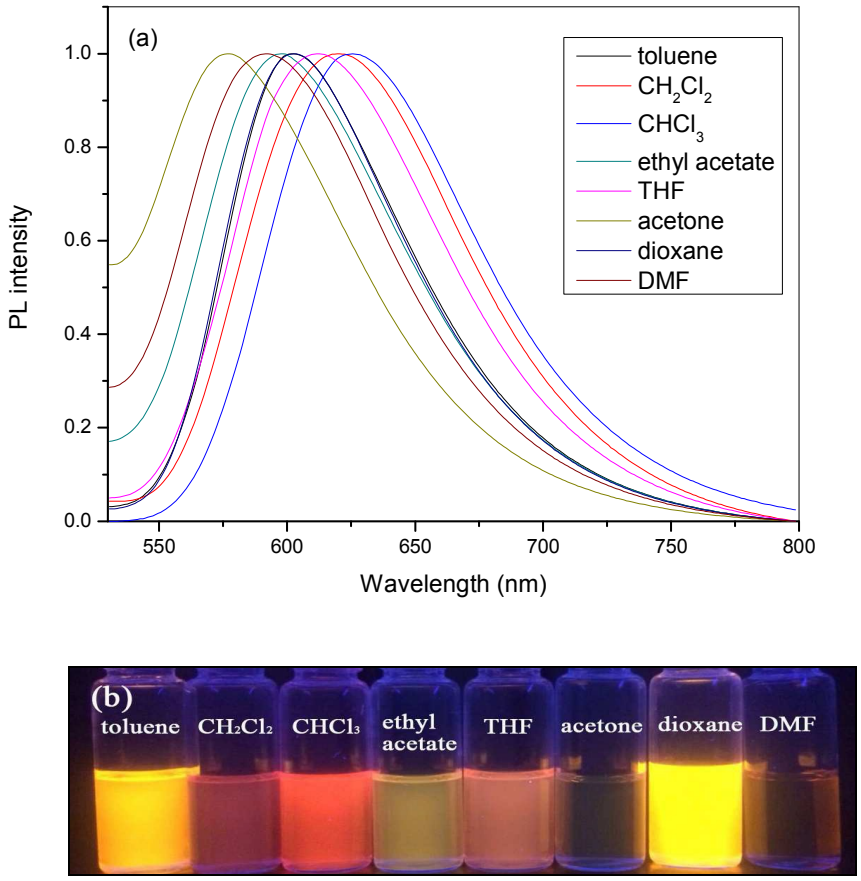

Fig. 3. (a) The normalized emission spectra of and (b) photographs of **N1** in different solvent under UV irridiation.

View Article Online
DOI: 10.1039/C6NJ00192K

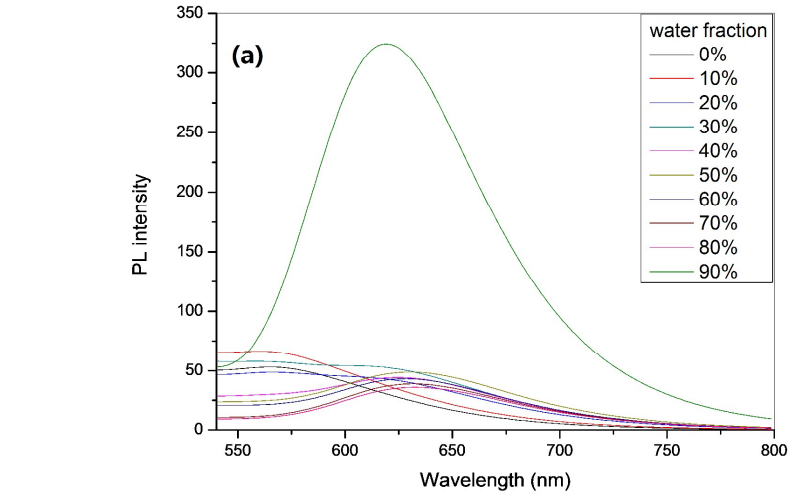

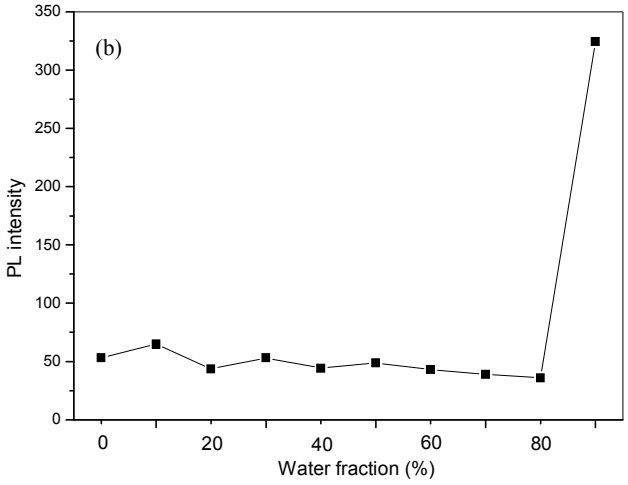

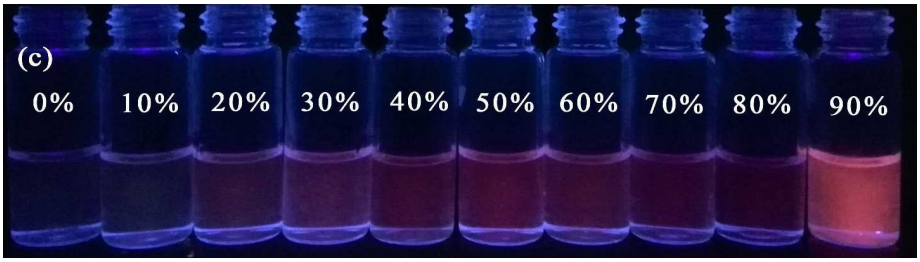

Fig. 4 (a) Emission spectra of **N1** (10 μM) in DMF/H_2O (λ_{ex} = 500 nm); (b) Plots of relative emission intensity enhancement factors *versus* water fractions; (c) Emission photographs of **N1** in DMF/H_2O mixtures with different water fractions at 365 nm UV irradiation.)

View Article Online
DOI: 10.1039/C6NJ00192K

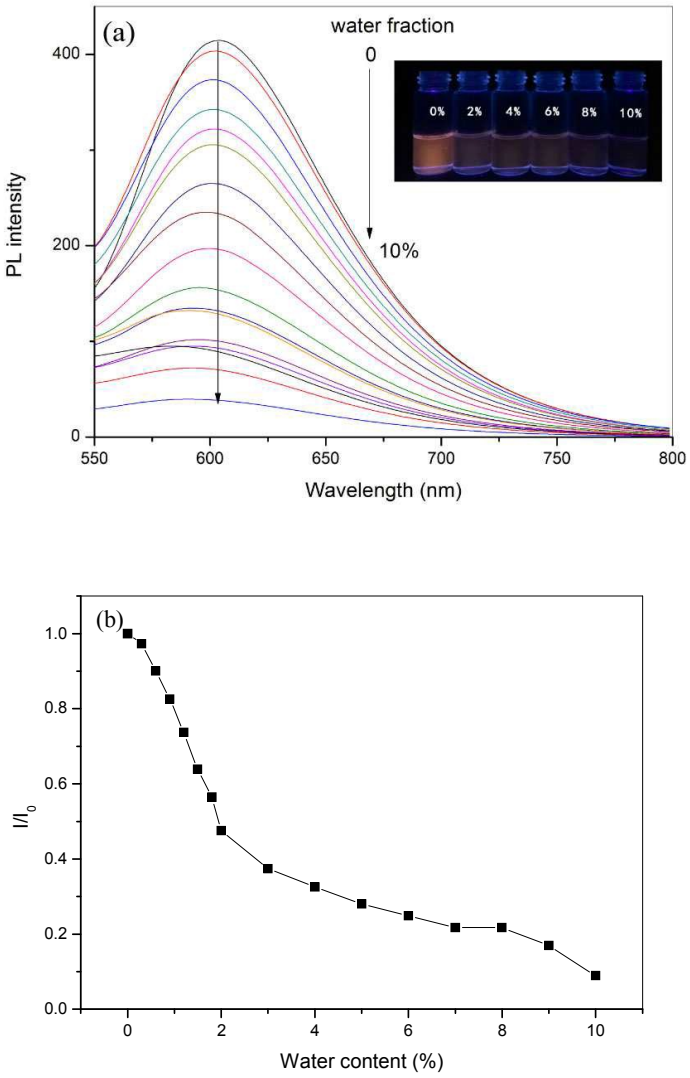

Fig. 5 (a) Emission spectra of **N1** (10 μM) in THF/H_2O (λ_{ex} = 500 nm); (b) Plots of relative emission intensity (I/I_0) *versus* water fractions.

View Article Online
DOI: 10.1039/C6NJ00192K

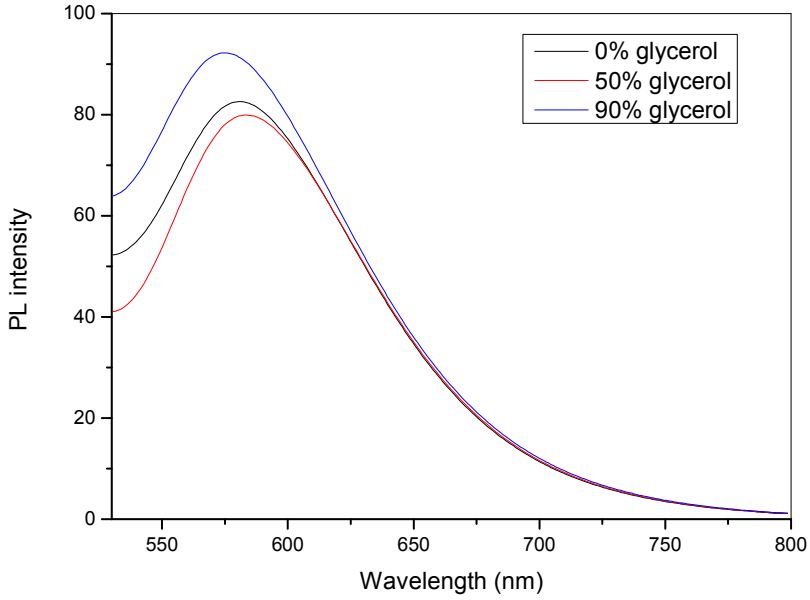

Fig. 6. Emission spectra of **P1** (20 μM) in various glycerol–DMSO mixture (λ_{ex} = 500 nm)

View Article Online
DOI: 10.1039/C6NJ00192K

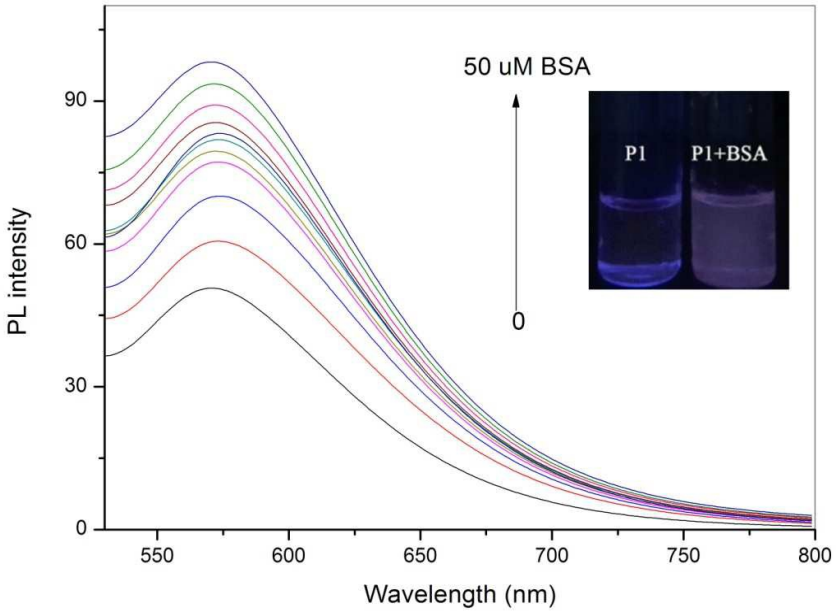

Fig. 7. Emission spectra of **P1** (20 μM) in various amount of BSA (λ_{ex}= 500 nm) in DMSO/PBS mixture (1:1, v/v). Inset: photogragh of **P1** in the presence and absence of BSA).

View Article Online
DOI: 10.1039/C6NJ00192K

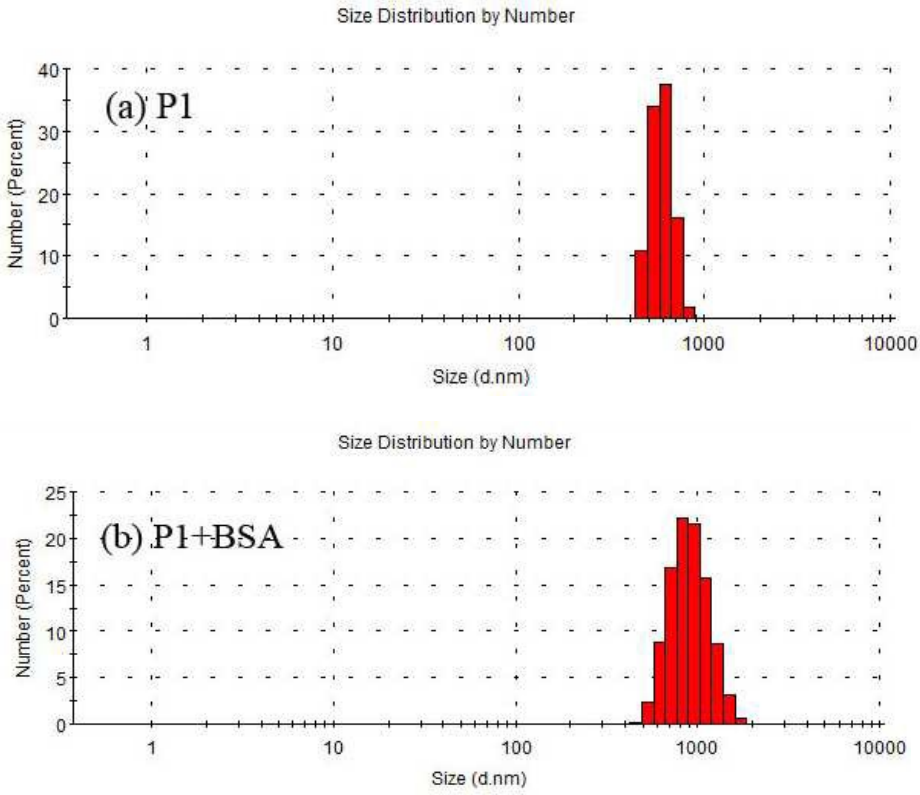

Fig. 8. Particle size distribution of **P1** (20 μM) in DMSO/PBS mixture (1:1, v/v) in the absence (a) and presence (b) of 50 μM BSA.

View Article Online
DOI: 10.1039/C6NJ00192K

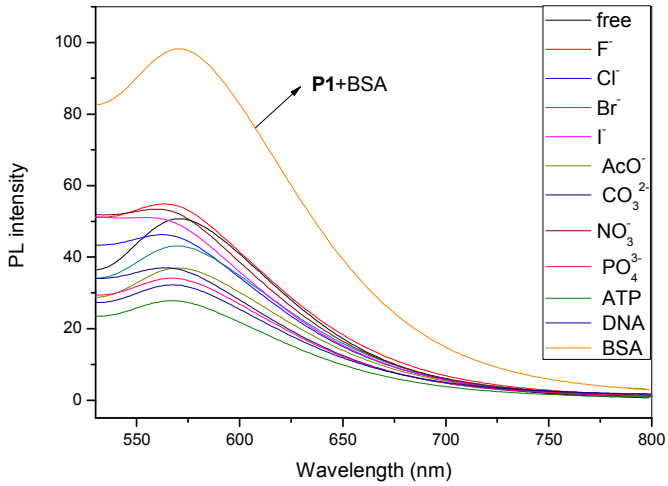

Fig.9 The fluorescence spectra of **P1** (10 μM) in presence of 50 μM DNA, ATP and anions.

View Article Online
DOI: 10.1039/C6NJ00192K

Graphical abstract

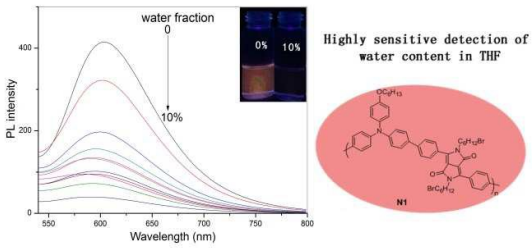

Polymer **N1** with solvatochromism and AIE features functions as a qualitative and quantitative probe for low-level water content in THF.